Layering in tailings deposits: Characterization and implications for CPT interpretation

Abideen T. Owolabi, MSc,[1] and Luis A. Torres-Cruz, PhD, MICE, CEng[2]

[1]PhD student, School of Civil and Environmental Engineering, University of the Witwatersrand, Johannesburg, South Africa. Email: toba2k74@gmail.com

[2]Assistant Professor, Norman B. Keevil Institute of Mining Engineering, University of British Columbia, Vancouver, Canada. Email: Luis.TorresCruz@ubc.ca

ABSTRACT

The cone penetration test (CPT) is widely used for tailings characterization. Often, the CPT is used to infer the state parameter (ψ) using methods based on uniform soil specimens. This paper addresses a crucial question: To what extent do tailings deposits resemble uniform specimens? We quantitatively characterized layering in tube samples from three active gold tailings storage facilities (TSFs) and visually appraised a 3 m profile at a fourth TSF. Results reveal pronounced thin layering in all samples and in the exposed profile. Our analysis suggests that the thickness of the uniform layers documented herein is less than 15 cm. This is significantly less than the >0.6 m thickness recommended for CPT interpretation. The PSD variability within a single 25 cm sample often matched or exceeded that observed across entire TSFs, highlighting the significance of the variability. Thin layering constitutes a significant deviation from the uniformity assumption that underpins widely used CPT interpretation methods and is likely to compromise the accuracy of CPT-based ψ estimates. Thin layering also raises fundamental questions about validating ψ estimates. We propose that tailings engineering would benefit from allowing more space for the approximate laboratory characterization of layered specimens rather than focusing on the precise characterization of uniform specimens that do not resemble in situ conditions.

1 INTRODUCTION

The cone penetration test (CPT) is likely the most widely used in situ geotechnical test to characterize tailings (Ayala et al., 2022; Fourie et al., 2022). Several CPT interpretation methods aim at inferring the state parameter (ψ) which is the void ratio (e) difference between a soil and its critical state line (CSL) at the current mean effective stress (p') (Been & Jefferies, 1985). The state parameter ψ is indicative of a soil's volume change tendencies at large strains and therefore of several aspects of engineering behavior. The first efforts to infer ψ from the CPT were based on data from calibration chamber (CC) testing supplemented by soil properties measured through triaxial testing (Been et al. 1986; 1987). CCs have a height and diameter of ~1 m and essentially allow a full-scale CPT to be performed in a laboratory environment in which soil characteristics, density, and stress levels can be controlled or measured.

CC tests and the supplementary laboratory testing use soil specimens that are as uniform as possible in terms of ψ as this is necessary to develop correlations with cone tip resistance. This translates to CC specimens with a uniform e and a constant particle size distribution (PSD), particle shape, and mineralogy to ensure a unique CSL. Techniques such as dry pluviation through sieves (Huntsman, 1985) or moist tamping after homogenization (Been et al., 1987) have been used to achieve the desired CC specimen uniformity. Similar approaches are used to achieve uniform triaxial specimens (Ayala et al., 2022; Been & Olivera, 2016; da Fonseca et al., 2021).

The framework proposed by Been et al. (1986; 1987) has been modified and expanded by numerous authors. Numerical simulations of cavity expansion, used as a CPT proxy, imply that the framework can now be implemented without having to perform CC tests (Shuttle & Jefferies, 1998). However, the newer methods are calibrated with CC results and retain the dependency on soil properties measured on uniform laboratory specimens (e.g., Shuttle & Cunning, 2007; Shuttle & Jefferies, 2016; Jefferies et al., 2019; Shuttle et al., 2022; Mozaffari & Ghafghazi, 2024) or estimated from CPT readings

48 (e.g., Plewes et al., 1992; Jung et al., 2025).

49 The widespread use in tailings engineering of the family of CPT interpretation methods that adopt
50 the Been et al. (1986; 1987) framework is reflected in the investigations of some of the most prominent
51 tailings storage facility (TSF) failures. For example, the investigations of TSF failures such as Samarco
52 (Morgenstern et al., 2016), Cadia Valley (Jefferies et al., 2019), and Brumadinho (Robertson et al., 2019;
53 CIMNE, 2021), collectively used the CPT interpretation methods described in Plewes et al. (1992), Shuttle
54 and Cunning (2007), and Shuttle and Jefferies (2016). The heavy reliance on this family of methods
55 prompts the question of the extent to which tailings deposits resemble the uniform CC and triaxial
56 specimens that underpin the framework. Layered deposits complicate CPT interpretation for at least two
57 reasons. Firstly, they constitute an important deviation from the conditions used to develop the Been et
58 al. (1986; 1987) framework. And secondly, in layered deposits multiple soils simultaneously affect cone
59 response (Boulanger & DeJong, 2018; Tehrani et al., 2017). Therefore, if a CPT interpretation method
60 requires soil properties, it is not clear which of the layered soils should be tested in the laboratory.
61 Furthermore, to the authors' knowledge, no studies have validated the use of homogenized sample
62 properties for CPT interpretation in layered tailings. Accordingly, it has been recommended that, to avoid
63 interference from adjacent layers, CPT interpretation should focus on layers that are >0.6 m thick and
64 have a stiffness ratio <5 between adjacent materials (Jefferies & Been, 2016). For instance, Shuttle and
65 Cunning (2007) reported CPT-based ψ estimates in a silt layer that was ~8 m thick and which exhibited
66 approximately constant values of a soil behavior type index derived from CPT readings. A unique set of
67 soil properties was assigned to this layer, implying that it was believed to be uniform.

68 Multiple works have incidentally or qualitatively reported tailings layering (Blight, 2010; da
69 Fonseca et al., 2020; Høeg et al., 2000; Jacobsz & Narainsamy, 2022; Vick, 1990). However, there is limited
70 literature focusing on quantitative characterization of such layering. For instance, Vermeulen (2001)
71 reported vertical profiles at a gold TSF that, based on color changes, exhibited layers that in some cases

were only a few centimeters thick. Reid et al. (2018a) reported gradation results of subaqueously deposited iron ore tailings and, based on the percentage passing the 38 and 75 µm sieves, found negligible signs of layering. Conversely, Reid et al. (2018c) sampled a surficial block of gold tailings and, based on the percentage passing the 75 µm sieve, identified layers that were smaller than ~30 mm. Reid et al. (2018c) noted that such layering poses a challenge to the application of critical state soil mechanics (CSSM). Reid and Fanni (2022) reported results from two block samples of iron ore tailings from which they extracted PSD specimens at ~2 cm intervals. Based on the percentages passing the 38 µm sieve, they reported modest PSD variations. However, it is inferred from Reid and Fanni (2022) that they made an effort to sample blocks that did not exhibit layering to enable comparisons between intact and reconstituted samples. Reid et al. (2022) examined block samples of gold, platinum and copper tailings. By considering the percentages passing the 38 and 75 µm sieves, they concluded that the blocks were layered and exhibited a wide range of gradations.

The reviewed literature suggests that while thick uniform tailings layers may exist in some TSFs, thinly layered structures can also develop. However, it is not clear how prevalent such layering is. Furthermore, investigations into tailings layering have described PSD curves with only one or two points. The importance of layering on CPT interpretation suggests that detailed PSD descriptions are warranted and are thus adopted herein. The authors were also unable to find any works that discuss the implications of tailings layering on CPT interpretation. Accordingly, this investigation characterized the layering in high-quality samples, sometimes referred to in the literature as undisturbed samples, from three active South African TSFs with varied hydraulic deposition methods. Additionally, a 3 m deep vertical profile at a TSF undergoing reclamation was visually appraised. The results are discussed within the context of CPT interpretation and alternative approaches to the mechanical characterization of tailings are suggested.

2 METHODOLOGY

2.1 Sites investigated

The fieldwork focused on gold tailings from the Witwatersrand Basin near Johannesburg, South Africa. Four upstream TSFs were investigated. Surficial high-quality samples that preserved the in situ layering were taken from three active TSFs, while visual inspections were performed at the fourth TSF. The three sampled TSFs were chosen to represent different depositional methods: cycloning, paddocking, and spigotting. Cycloning uses hydrocyclones to separate the tailings feed into a coarse fraction (underflow) and a fine fraction (overflow) deposited on the outer and internal part of the TSF, respectively. Paddocking involves depositing tailings in enclosed areas (the paddocks) on the crest of the dam during the day and depositing in the internal part of the TSF at night. Spigotting uses outlets or spigots connected to a main delivery pipe that runs along the perimeter of the outer wall of the TSF. Detailed descriptions of these methods have been previously reported (Blight, 2010; McPhail & Wagner, 1987). Hereafter, the three sampled TSFs will be referred to simply as the Cyclone TSF, Paddock TSF, and Spigot TSF. The fourth investigated TSF was undergoing reclamation to enable tailings reprocessing and this allowed inspection of layering patterns along profiles that were several meters long. This TSF also adopted paddocking deposition and will be referred to as the Remine TSF. Figure 1 shows the locations of the TSFs and Figure 2 shows their overall layout.

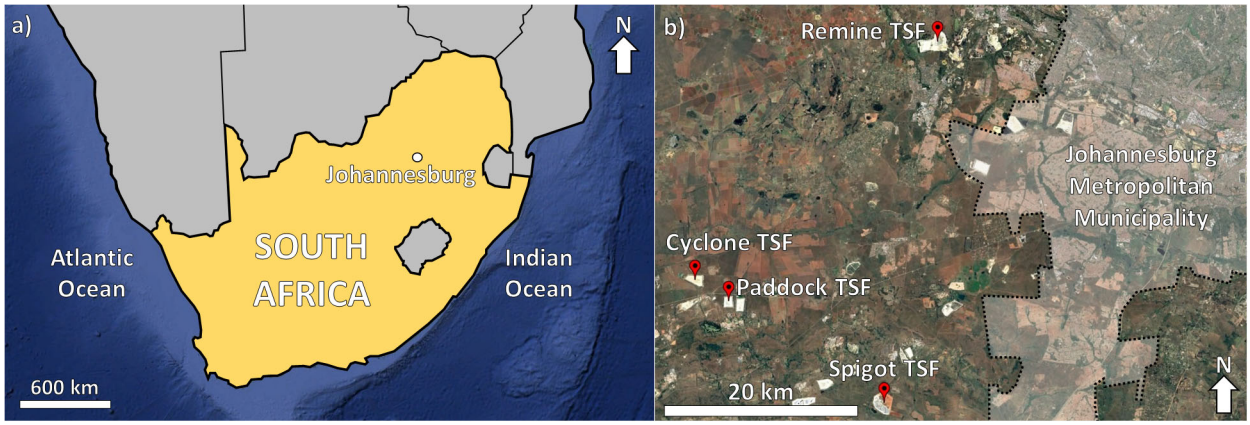

Fig. 1. Location of the TSFs: a) Location of Johannesburg within South Africa and b) Location of the TSFs with respect to Johannesburg. Source: Google Earth Pro.

2.2 Sampling and characterization of tailings

A stainless-steel split tube sampler (Figure 3) was manufactured to extract surficial samples that preserved any potential layering. The sampler meets the requirements of ASTM D1587-15 (ASTM, 2015) and is similar to a sampler previously used for gold tailings (Vermeulen, 2001). The upper portion of the sampler consists of a split solid cylinder that has a 1 mm diameter vent hole through its center. The hole also enabled the insertion of a 0.75 mm rod used to check that the sampler was full. The sampling tube is 250 mm long with inner and outer diameters of 75 and 80 mm. The lowest 25 mm of the sampling tube are tapered at 5° to facilitate sampling. The tube was polished inside and out to minimize friction.

The entire length of the sampling tube was pushed into the tailings from surface level. To minimize disturbance, the sampler was then dug out rather than pulled out. Subsequently, the sampler was opened and the sample marked at 1 cm intervals to obtain 25 slices (Figure 4). A cutting plate was then used to slice the sample and each slice was stored in a labelled, air-tight bag for transportation to the laboratory. For each sample, the slices were numbered from 1 to 25 from top to bottom. To achieve a uniform slicing frequency, the slices were always cut at 1 cm intervals regardless of the layer boundaries suggested by color changes. However, assuming that color changes reflect alterations in PSD and mineralogy, some

133 layers could have been thinner than 1 cm (e.g., the lowest three centimeters of the sample in Figure 4).

134

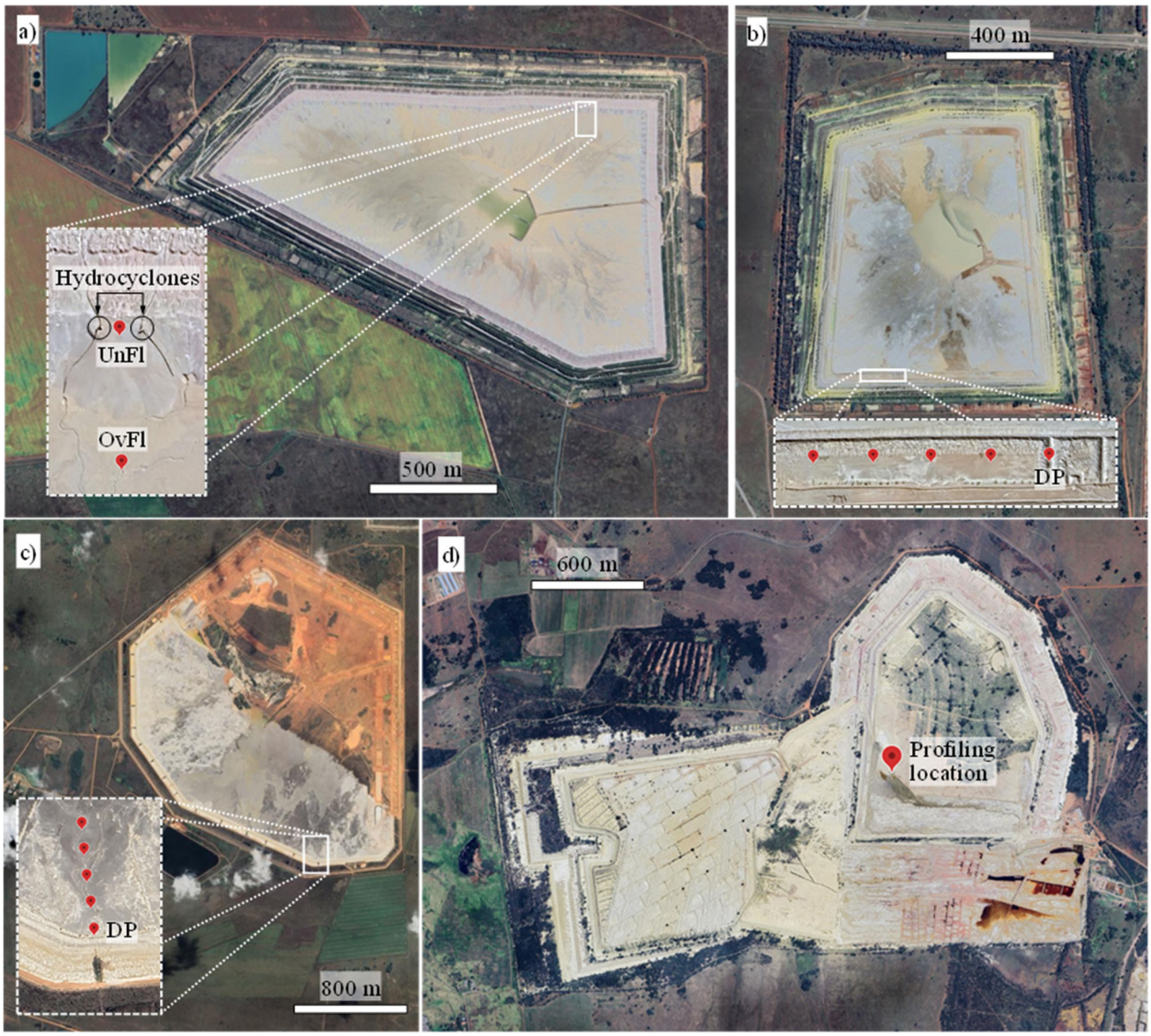

135

136 **Fig. 2.** Satellite images of the investigated TSFs: a) Cyclone TSF; b) Paddock TSF; c) Spigot TSF; and d)

137 Remine TSF. Notes: Insets in parts a) to c) show sampling locations. OvFl = overflow; UnFl = underflow, DP

138 = Discharge point (not sampled). Source: Google Earth Pro.

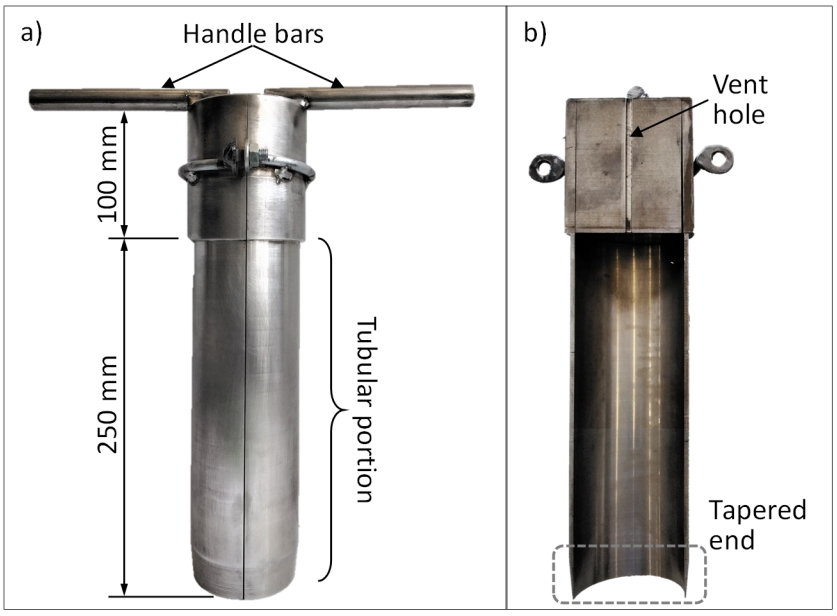

Fig. 3. Tailings sampler: a) assembled and b) internal lateral view.

Fig. 4. Sample 'Spigot @100' with marks at 1 cm intervals prior to being sliced.

Ten samples, resulting in 250 slices, were collected from the locations shown in Figure 2. At the Cyclone TSF, both the underflow and the overflow were sampled. And for the Paddock and Spigot TSFs samples were collected at different distances from the discharge point. Table 1 provides additional details regarding the sampling locations and the code used to identify each sample. The code is composed of the

name of the TSF and an indication of the distance from the discharge point or, in the case of the Cyclone TSF, of whether the sample was of the underflow or overflow. Individual slices will be identified herein by adding the slice number to the code of the sample. For instance, slice *Cyclone UnFl (7)* is the seventh slice from top to bottom of the underflow sample at the Cyclone TSF.

The particle shape of the tailings from the three sampled TSFs was examined using scanning electron microscopy (SEM) on three tailings size fractions isolated by sieving (>150 µm, 75 to 150 µm, and <75 µm). The particles were highly angular regardless of particle size (Figure 5), which is characteristic of tailings generated from ore crushing (e.g., Torres-Cruz & Santamarina, 2020; Vermeulen, 2001).

Table 1. Location and code of the ten samples recovered with the tube sampler.

TSF	**Location**	**Code**
Cyclone	9 m along outer wall from underflow discharge (Figure 2a).	Cyclone UnFl
	35 m towards the decant pond from overflow discharge (Figure 2a).	Cyclone OvFl
Paddock	25, 50, 75, and 100 m from discharge within the paddock (Figure 2b).	Paddock @25, Paddock @50, Paddock @75, Paddock @100
Spigot	25, 50, 75, and 100 m from discharge towards the decant pond (Figure 2c).	Spigot @25, Spigot @50, Spigot @75, Spigot @100

The mineralogy of one slice from each sampled TSF was analyzed using X-ray diffraction. The analyzed slices exhibited a PSD that was deemed representative of the respective TSF. Table 2 summarizes the mineralogy and shows that the tailings from all three TSFs are dominated (>55%) by quartz. This agrees

with previous reports of the mineralogy of gold tailings from the Witwatersrand Basin (Chang, 2009; Vermeulen, 2001). The tailings also contained significant amounts (> 8%) of chlorite. Additionally, the Paddock TSF exhibits significant amounts (> 8%) of plagioclase, muscovite, and actinolite.

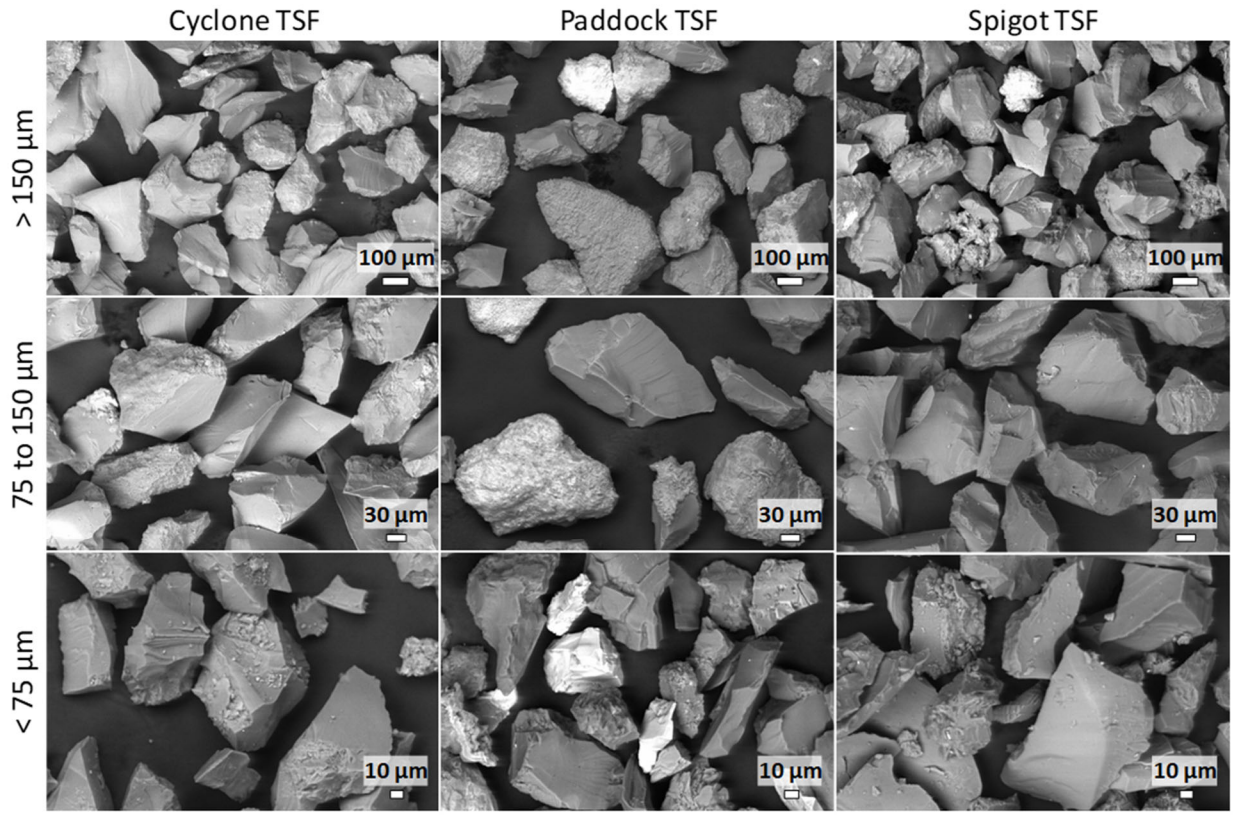

Fig. 5. Scanning electron microscopy images of the sampled tailings.

The specific gravity (G_s) was measured following BS 1377:2 (BSI, 1990) for the finest and coarsest slice encountered at each TSF. For the Cyclone TSF and the Paddock TSF the G_s was 2.70 and 2.72, respectively, for both slices. For the Spigot TSF the fine slice yielded 2.59 and the coarsest 2.67. These results are consistent with the quartz-dominated mineralogy (Table 2) and previous G_s values reported for gold tailings (Chang, 2009; Vermeulen, 2001).

Table 2. Mineralogy of the three sampled TSFs.

Mineral	Cyclone OvFl (2)	Paddock @25 (17)	Spigot @100 (8)
Quartz	77.5	56.4	74.6
Plagioclase	0	8.9	0
Chlorite	8.4	8.5	8.6
Microcline	0	1.6	0
Muscovite	4.6	8.1	3.2
Pyrophyllite	2.9	4.5	5.8
Talc	0	0	5.3
Hematite	0.6	0	0
Chloritoid	4.0	0	0
Pyrite	0	0	0.7
Dolomite	0	2.9	0
Gypsum	2.0	0	0
Actinolite	0	9.1	0
Calcite	0	0	1.8

In order to assess variability along the length of the samples, the PSD and plastic limit (PL) of each slice were determined. PSDs were measured with a laser diffraction spectroscopy device (Anton Paar PSA 1090) which operates on particle sizes ranging from 0.04 to 500 μm. The specimen mass required for the PSD determinations ranged between 0.9 and 1.4 g. Each PSD specimen was extracted from the central portion of the top surface of each slice. The dispersing agent was sodium hexametaphosphate (5 g/liter) as per ASTM D7928-21 (ASTM, 2021). The specimens and the dispersing solution were placed in a covered container and left overnight in the temperature-controlled room that housed the laser diffraction device

185 to ensure temperature equilibrium and promote deflocculation. PL determinations followed the thread
186 rolling method of BSI 1377:2 (BSI, 1990). Additional index properties, such as the liquid limit or the
187 minimum and maximum void ratio were not determined due to the limited mass of each slice.
188
189 **2.3 Profiling at the Remine TSF**
190 The reclamation activities at the Remine TSF allowed us to expose a 3 m deep profile for visual
191 appraisal at the location shown in Figure 2d. To this end, we adopted an approach similar to that described
192 in Vermeulen (2001). Six 0.5 m tall benches were created by cutting into the tailings with the flat blade of
193 a spade. The vertical faces were then individually photographed.
194
195 **3 RESULTS**
196 **3.1 Layering characteristics in the sampled tailings**
197 Figures 6 to 8 show the 25 PSDs measured on each sample collected at the Cyclone, Paddock, and Spigot
198 TSFs. At the Cyclone TSF, the range of gradations is broader for the underflow sample than for the
199 overflow sample (Figure 6). At the Paddock TSF, the samples collected 25 and 50 m away from the
200 discharge point exhibited the broadest range of gradations. Whereas the samples collected 75 and 100 m
201 away from the discharge point exhibited narrower and finer gradations. This is consistent with the general
202 trend of coarser particles settling out of the slurry closer to the discharge point (Blight, 2010). As for the
203 Spigot TSF, the sample collected at 100 m from the discharge point exhibited the broadest range of
204 gradations. The four Spigot TSF samples do not reveal a clear trend of PSDs becoming finer as the distance
205 from the discharge point increases. This is not entirely surprising, as data from Blight (2010) suggests that
206 in some cases it is necessary to collect samples over longer distances along the beach for clear PSD trends
207 to emerge.
208 To provide context, Figures 6 to 8 include the PSD envelopes of two TSFs that failed in Brazil: The

209 Samarco TSF (Rezende, 2013) and the Córrego do Feijão TSF (Robertson et al., 2019). The Samarco TSF
210 failure is also widely referred to by the name of the containment structure that failed which was the
211 Fundão Dam. And the Córrego do Feijão TSF failure is better known by the name of the nearby town,
212 Brumadinho. PSD data representative of the tailings contained by the Fundão Dam were obtained from
213 Rezende (2013) because this source was relied upon during the post-failure investigation (see Appendix
214 D in Morgenstern et al. 2016). The PSD envelope for Fundão is based on 26 samples of which 18
215 correspond to the tailings slurry as it leaves the concentration plant, and 8 correspond to samples taken
216 over a 110 m distance that stretched from the dam crest into the tailings beach (Rezende, 2013). The PSD
217 range for the Brumadinho TSF is based on 20 samples described as coarse, fine, or berm fill tailings in
218 Robertson et al. (2019). The samples from both TSFs aimed at characterizing the different types of
219 impounded tailings.

220 The PSD envelopes of the Fundão and Brumadinho PSDs are generally coarser than the PSDs
221 measured in our ten samples. Accordingly, to facilitate the comparison of the spread of the PSDs, the
222 reference envelopes were shifted to the left by dividing all the particle sizes of the envelopes by a number
223 which varies across plots and is indicated in the legends of Figures 6 to 8. Because the horizontal axis is
224 logarithmic, this division does not alter the shape of the envelopes.

225 Figures 6 to 8 show that the range of PSDs in a single 25 cm sample is often comparable, and
226 sometimes even larger, than the PSD envelopes. This is particularly true when comparing the sample PSDs
227 to the Fundão PSD envelope which is narrower than that at Brumadinho. However, even the wider range
228 of the Brumadinho PSD envelope is similar to the PSD variability of some samples (Figure 7a, b and Figure
229 8d). It seems likely that if the PSD samples at Brumadinho and Fundão had been subjected to the detailed
230 slicing adopted herein, their PSD envelopes would have been wider. Notwithstanding, Figures 6 to 8 show
231 that the PSD variability that occurs along a small 25 cm sample is not merely a minor deviation from a
232 central trend, but rather a variability that is comparable to that observed across an entire tailings

impoundment.

Figure 9 shows profiles of D_{10}, D_{50}, and D_{90} along the height of the ten samples. The plots further highlight how changes in gradation occur over centimeters. The profiles suggest that the thickest uniform layer in all ten samples corresponds to the upper ~15 cm of the Cyclone OvFl sample (Figure 9b). This is consistent with the narrower band of PSDs observed in Figure 6b.

Plastic limits (PL) could not be measured for the large majority of the slices because the nonplastic nature of the tailings prevented them from being rolled into threads. Table 3 summarizes the limited PL results obtained. All values fall within a relatively low and narrow range of 23% and 33%. This suggests that while PSD varied significantly within the samples, plasticity did not.

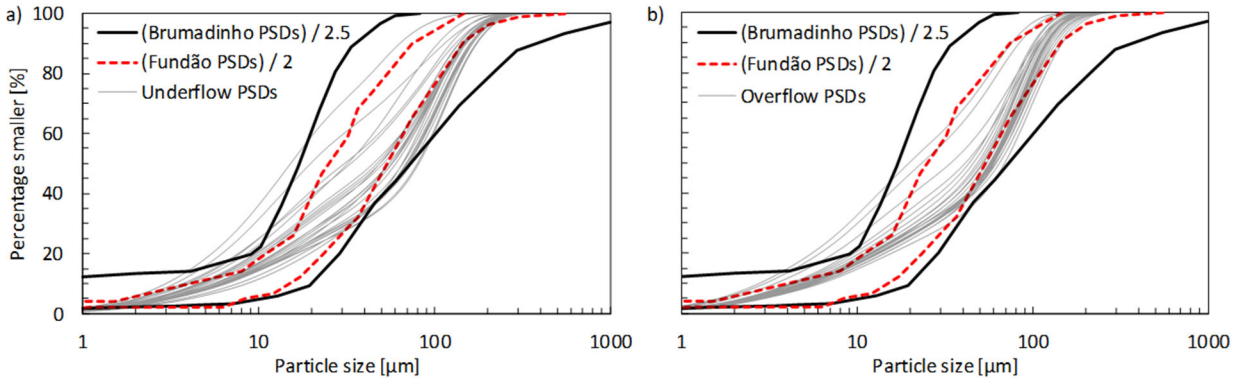

Fig. 6. Range of PSDs in the samples: a) Cyclone UnFl and b) Cyclone OvFl. Note: Laterally shifted PSD envelopes shown for Fundão (Rezende, 2013) and Brumadinho (Robertson et al., 2019).

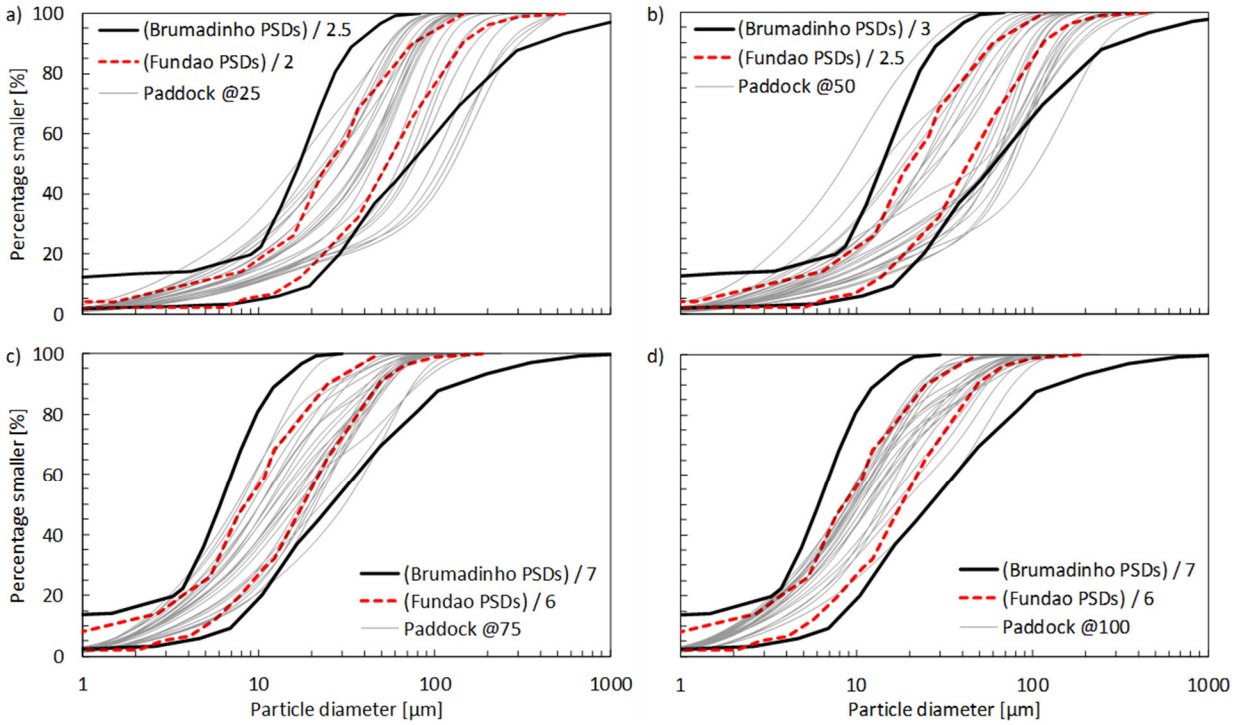

247

248 **Fig. 7.** Range of PSDs in the samples: a) Paddock @25, b) Paddock @50, c) Paddock @75, and d) Paddock

249 @100. Note: Laterally shifted PSD envelopes shown for Fundão (Rezende, 2013) and Brumadinho

250 (Robertson et al., 2019).

251

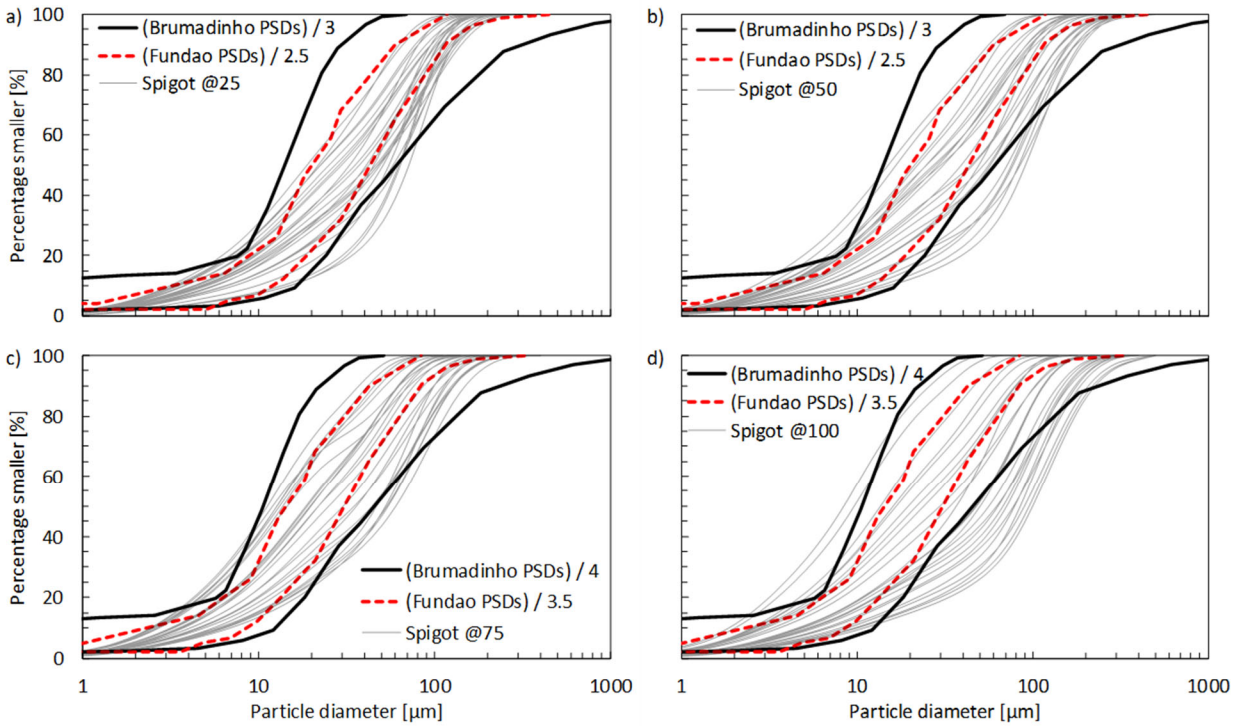

252

253 **Fig. 8.** Range of PSDs in the samples: a) Spigot @25, b) Spigot @50, c) Spigot @75, and d) Spigot @100.

254 Note: Laterally shifted PSD envelopes shown for Fundão (Rezende, 2013) and Brumadinho (Robertson et

255 al., 2019).

256

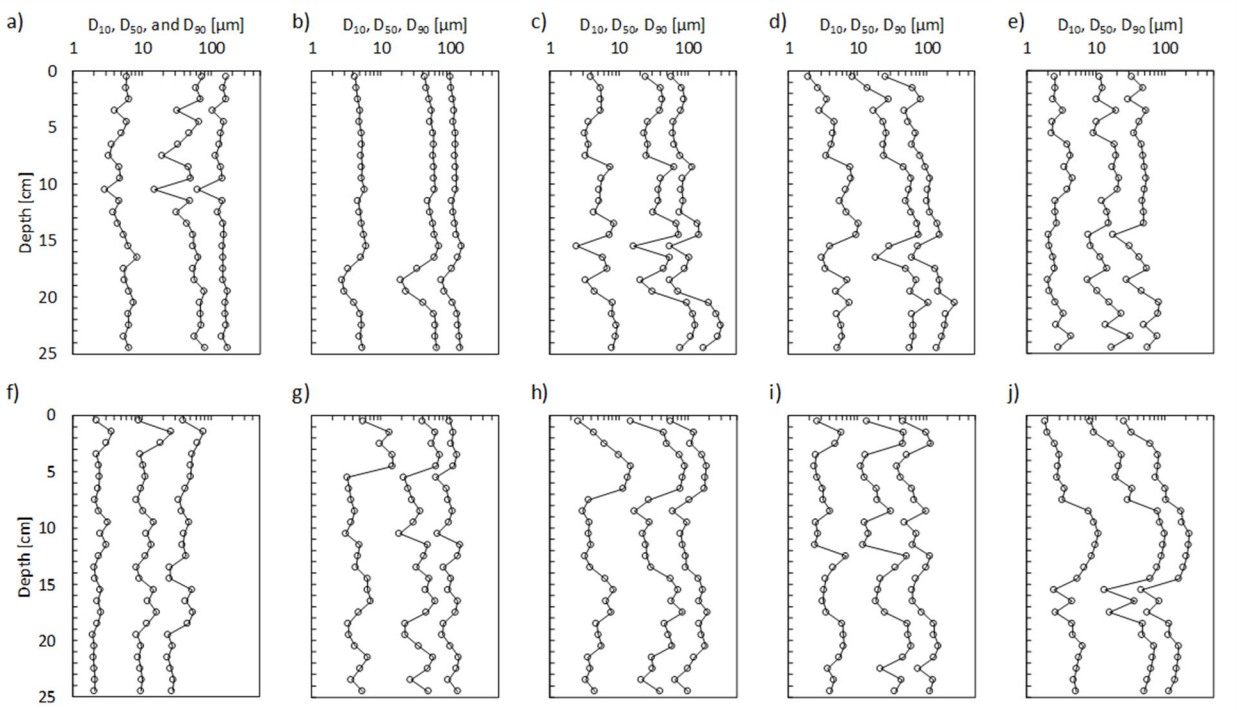

257

258 **Fig. 9.** Profiles of D_{10}, D_{50}, and D_{90} of samples a) Cyclone UnFl, b) Cyclone OvFl, c) Paddock @25, d) Paddock

259 @50, e) Paddock @75, f) Paddock @100, g) Spigot @25, h) Spigot @50, i) Spigot @75, and j) Spigot @100.

260

261 **Table 3.** Plastic limit results.

TSF	Sample	Slice numbers	PL Range (%)
Paddock	Paddock @ 50m	1 – 2	23 – 27
	Paddock @ 75m	2 – 4 and 13 – 20	24 – 32
	Paddock @ 100m	3 – 15	24 – 33
Spigot	Spigot @ 75m	5 – 7	27 – 32
	Spigot @ 100m	1 – 2	30 – 33

262

3.2 Layering in the exposed profile of the Remine TSF

Figure 10 shows the 3 m profile exposed at the Remine TSF. Assuming that changes in color reflect changes in mineralogy or PSD, the thinly layered nature of the tailings deposit is evident. Several portions exhibit layers that are only a few millimeters thick (e.g., between 20 and 40 cm, 130 and 140 cm, and 170 and 180 cm). Overall, Figure 10 suggests that uniform layers are unlikely to exceed thicknesses of ~10 cm.

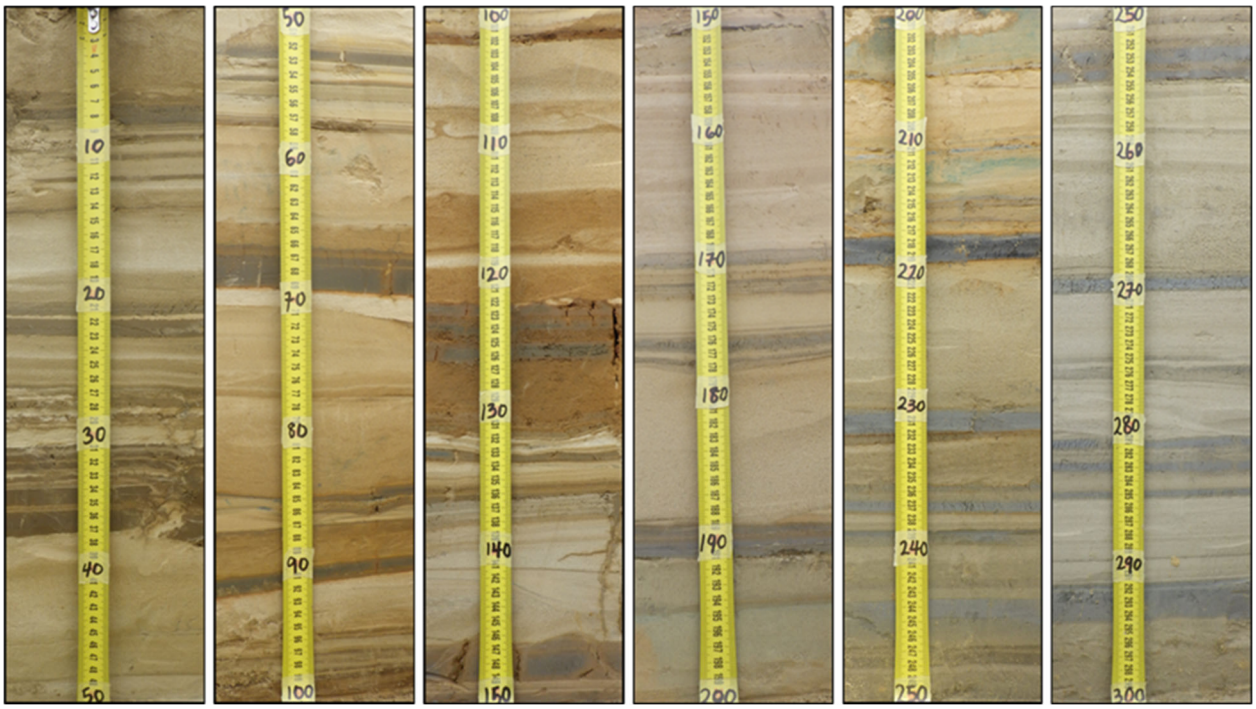

Fig. 10. The 3 m deep profile at the Remine TSF. Note: The measuring tape shows centimeters.

4 DISCUSSION

4.1 Implications for CPT interpretation

The thin layering of the four tailings deposits constitutes a significant deviation from the uniform CC and triaxial testing specimens that underpin the CPT interpretation methods based on the Been et al. (1986; 1987) framework and which include some of the most widely-used methods in TSFs (e.g., Jefferies et al., 2019; Jefferies & Been, 2016; Jung et al., 2025; Plewes et al., 1992; Mozaffari & Ghafghazi, 2024; Shuttle

& Cunning, 2007; Shuttle & Jefferies, 1998; Shuttle & Jefferies, 2016; Shuttle et al., 2022). Our findings are consistent with thin layering reported in hydraulically deposited tailings from gold (Vermeulen, 2001) and other commodities (Reid et al., 2018c, 2022). This thin layering, often underexplored quantitatively, raises questions about the suitability of the Been et al. (1986; 1987) framework to characterize hydraulically deposited tailings.

Furthermore, some of the methods based on this framework require soil properties that have to be measured through laboratory testing such as the slope of the CSL in e-logp' space (λ), dilation properties, plastic parameters, and elastic parameters (e.g., Ayala et al., 2022; Robertson et al., 2019; Shuttle et al., 2022). While PSD may not significantly affect soil properties in some cases (Robertson et al., 2019), it generally affects at least the CSL slope λ and the state-dilatancy property X_{tc} (Jefferies & Been, 2016; Torres-Cruz, 2021). Accordingly, the standing recommendation is to assume that different PSDs yield different properties that have to be characterized independently (Jefferies & Been, 2016). Characterizing multiple PSDs, as done in the Cadia Valley and Brumadinho investigations (Jefferies et al., 2019; Robertson et al., 2019), is consistent with the presence of varied gradations within a single TSF. However, this does not address the challenge posed by thinly layered deposits in which several soils simultaneously affect the CPT response, making it unclear which soil properties should be used for CPT interpretation. That is, the practicing engineer is left unsure about which tailings gradation should be sent to the laboratory for detailed testing or if a homogenized sample will yield adequate results. And although ψ variations were not explored herein, it is also possible for ψ to vary across layers, constituting a further deviation from the uniform CC and triaxial specimens.

Considering the potentially catastrophic consequences of TSF failures, the validation of any approach aimed at making in situ estimates of ψ should ideally be based on blind predictions compared against high-quality specimens from sites at which the vertical and horizontal effective stresses have been measured. This latter requirement arises from the need to compute p' in order to calculate ψ. To test the

robustness of the method, the validation should cover a wide range of ψ values and involve multiple teams working independently from each other. However, thin layering poses a fundamental challenge to this hypothetical validation scheme because changes in PSD can affect the height of the CSL in *e*-log*p*′ space (Thevanayagam et al., 2002; Torres-Cruz, 2019). Accordingly, if a high-quality layered sample is obtained to confirm a CPT-based ψ estimate, it is not clear which is the CSL that should be used to compare against the overall void ratio of the sample (e.g., Jefferies et al., 2019).

Of the multiple CPT interpretation methods based on the Been et al. (1986; 1987) framework, the "widget" method, which is anchored on CSSM and was developed by Shuttle and Cunning (2007), Shuttle and Jefferies (2016), Jefferies et al. (2019), and Shuttle et al. (2022), appears to be the most highly regarded in the tailings industry. For instance, the method was used to investigate the failures at Brumadinho and Cadia Valley (CIMNE, 2021; Jefferies et al., 2019; Robertson et al., 2019). Notwithstanding, using data from three TSFs, comparisons between ψ as measured in "undisturbed" samples and ψ as inferred from the widget method show a lack of overall agreement (Fourie et al., 2022). It should be noted that the ψ comparisons reported by Fourie et al. (2022) do not meet the standards of the ideal validation scheme described above but appear to be the only data available to make this type of comparison. The results reported herein suggest that thin layering of tailings may be contributing to the lack of agreement. It has also been suggested that the discrepancy could be due to the fact that the CC testing that underpins the widget method includes predominantly dilatant sands unlike the contractive soils that are of greatest geotechnical interest (Ayala et al., 2022).

Our results challenge what appears to be a widely held view that the Been et al. (1986; 1987) framework is currently the most promising approach for tailings characterization. For instance, recent guidelines on tailings dam safety issued by the International Commission on Large Dams (ICOLD, 2025) note that high-quality specimens provide the most reliable method of directly measuring in situ void ratio "but may be extremely costly", "impossible" and "are often unreliable" due to disturbance. Accordingly,

the ICOLD guidelines go on to say that the "CPTu currently provides the most practical means to infer the in situ state of many soils, especially tailings" and note that Jefferies and Been (2016), which adopts the Been et al. (1986; 1987) framework, describes correlations to estimate ψ. It seems reasonable to expect that upon reading this guidance most engineers will be discouraged from attempting to pursue testing on high-quality specimens and will rather rely on the Jefferies & Been (2016) approach. A decision which, as discussed below, precludes the possibility of gaining useful insights from testing high-quality specimens or may lead to an unwarranted discarding of results from more empirical CPT interpretation methods.

4.2 Suggestions for the path forward

The search of alternatives to the Been et al. (1986; 1987) framework leads to more empirical CPT interpretation methods that are directly based on the back analysis of TSF failure case histories. Such methods include those proposed by Olson and Stark (2001, 2002), Robertson (2016, 2022) and Sadrekarimi (2014). While these methods also have their limitations (Fourie et al., 2022), their empiricism appears to be consistent with our current limited ability to characterize thinly layered deposits. Of note, empirical CPT interpretation methods are also recommended in the abovementioned ICOLD (2025) guidelines. The guidelines correctly note that implementation of the Jefferies and Been (2016) approach requires a significantly higher effort than the empirical methods and that this higher effort is generally justified for TSFs with potentially catastrophic consequences of failure. The implication is that the Jefferies and Been (2016) approach yields more accurate results than the empirical methods. A claim which, to our knowledge, lacks supporting experimental data. We hypothesize that the theoretical grounding provided by CSSM, combined with its complex numerical implementation and extensive laboratory testing requirements may lead to an overestimation of the accuracy of the Jefferies and Been (2016) approach. This concern may also apply more broadly to other approaches that adopt the Been et al. (1986; 1987) framework. Furthermore, while the CPT remains the most widely used test for the mechanical

characterization of tailings, alternative geotechnical and geophysical in situ tests can also play an important role in helping the profession find the answers it seeks (e.g., Fourie et al., 2022; Schnaid, 2020).

It was noted above that several soil properties used in methods that adopt the Been et al. (1986; 1987) framework depend on PSD. However, there is at least one soil property that does not have a strong PSD dependence and which may be useful in finding a path forward. The critical state friction ratio measured under triaxial compression conditions (M_{tc}) remains virtually constant across different PSDs from the same TSF (Bandini and Coop, 2011; Carrera et al., 2011; Torres-Cruz & Santamarina, 2020). This appears to be due to the strong dependence of M_{tc} on particle shape (Sadrekarimi and Olson, 2011) which in crushed-ore tailings remains highly angular over most particle sizes (Figure 5; Torres-Cruz & Santamarina, 2020; Vermeulen, 2001). It seems likely that properties that show limited PSD dependence are good candidates to aid the robust characterization of layered tailings.

Considering the significant laboratory testing effort involved in obtaining precise CSSM parameters of uniform specimens that may not be representative of in situ conditions, the tailings profession should consider whether more value could be gained from characterizing high-quality specimens that try to preserve the in situ thin layering and fabric. Testing high-quality specimens is likely to result in a more approximate characterization because differences among such specimens will be more pronounced than differences between reconstituted specimens and this introduces scatter. Notwithstanding, the literature shows that, despite current limitations in obtaining high-quality specimens, they can play an important role in understanding tailings behavior. For instance, Høeg et al. (2000) reported comparisons of the triaxial compression behavior of undisturbed and reconstituted specimens of copper tailings from the Zelazny Most TSF. The undisturbed specimens were dilatant whereas denser reconstituted specimens were contractive. Høeg et al. (2000) suggested that this was predominantly due to differences in fabric although they indicated that the pronounced layering of the undisturbed tailings may have also played a role. Consequently, Høeg et al. (2000) concluded that the

374 results of the reconstituted specimens should not be used in the analyses of the Zelazny Most TSF.
375 Additional comparisons between undisturbed and reconstituted specimens from the Zelazny Most TSF
376 presented by Jamiolkowski (2014) yielded similar results: at the same void ratio the large strain behavior
377 of undisturbed specimens was dilative while that of reconstituted specimens was contractive. Accordingly,
378 Jamiolkowsky (2014) concluded that the Zelazny Most tailings were barely susceptible to flow failure. In
379 an unrelated investigation, Fourie et al. (2001) used ground freezing to recover undisturbed specimens of
380 oil sand tailings from below the phreatic surface and found, via physical measurements, gas
381 chromatography and microscopy analyses, that the specimens were not fully saturated. Fourie et al.
382 (2001) noted that this partial saturation may reduce the liquefaction potential of tailings sand under
383 undrained loading and that, while it was premature to modify engineering practice on the basis of their
384 observations, this was an issue that required further investigation. In two different examples, high-quality
385 surficial tailings specimens were used in monotonic direct simple shear testing to characterize the peak
386 undrained strength ratio induced by desiccation (Reid et al. 2018b, c). The tests enabled the estimation of
387 the preconsolidation pressures induced by sun drying. Similarly, an investigation into the Brumadinho TSF
388 failure used high-quality specimens to estimate in situ physical, hydraulic, and geomechanical parameters
389 (da Fonseca et al., 2020). It is clear that although the testing of high-quality tailings specimens currently
390 appears to only play a modest role in geotechnical characterization, there are useful insights that can be
391 gained from it.

392 The prospect of testing undisturbed specimens brings to the fore concerns about the fact that
393 such specimens are not truly undisturbed, as some disturbance is expected during the extraction,
394 transportation and mounting processes. This is particularly true for nonplastic granular media such as
395 many types of tailings. The authors hope that greater awareness of the stark differences between the
396 thinly layered structure of hydraulically deposited tailings and the uniform specimens that underpin some
397 of the most widely used CPT-interpretation methods will prompt greater interest in developing and

validating high-quality sampling techniques. It is worth noting that a recent survey about the expectations of tailings engineers for the year 2030 found that one of the points of interest was the development of better undisturbed sampling methods for fine and coarse tailings (Small et al., 2024). An interesting development aimed at enabling the laboratory testing of high-quality specimens, but not directly related to the improvement of sampling techniques, is an industrial-academic collaboration in South Africa to develop a state-of-the-art mobile (truck-mounted) geotechnical laboratory (UP, 2023). By taking the laboratory to the TSF, the specimen disturbance due to transportation is significantly reduced. The authors are not aware of mobile tailings laboratories elsewhere and posit that there could be significant advantages in further exploring this approach.

5 CONCLUSIONS

Current tailings engineering practice emphasizes the inference of the state parameter ψ from CPT results which are often supplemented by laboratory testing. The quest for ψ is understandable as it helps predict the drained and undrained large-strain behavior of saturated tailings (Been & Jefferies, 1985). However, several widely used CPT interpretation methods are based on CC and triaxial testing of uniform specimens. This raises the question of whether tailings deposits resemble these uniform specimens.

This work documented the layering characteristics of four hydraulically deposited gold TSFs. Ten tube samples that were 25 cm long were extracted from three of the TSFs for laboratory index testing. Additionally, a 3 m deep profile at the fourth TSF was visually appraised for color changes hypothesized to correspond with changes in PSD or mineralogy. Thin layering, albeit with consistently low plasticity, was observed in all ten tube samples and in the 3 m deep profile, with PSD variability in some samples matching or exceeding the variability observed at entire TSFs. This layered structure, which appears to be common in hydraulically deposited tailings from other commodities (Reid et al., 2022), contrasts starkly with the uniform specimens used in the CC and triaxial testing that underpin several widely used CPT

interpretation methods.

The thin layering documented herein is also at odds with a published recommendation to focus CPT interpretation on layers exceeding 0.6 m (Jefferies & Been, 2016). In contrast, the samples and profile examined herein suggest that the thickest uniform layer did not exceed ~0.15 m. These observations raise questions about the fundamental compatibility between CPT interpretation methods based on uniform specimens, and thinly layered deposits. This potential incompatibility may be contributing to known limitations in CPT-based ψ estimates, such as those reported for the widget method (Fourie et al., 2022).

Considering that current practice is strongly dominated by the laboratory testing of reconstituted uniform specimens to obtain precise CSSM parameters, we propose that there should be more space for the approximate characterization of high-quality specimens that preserve their in situ layered structure. This would be in line with the principle that "it is better to be vaguely right than exactly wrong" (Read, 1920).

6 DATA AVAILABILITY STATEMENT

All data, models, and code generated or used during the study appear in the submitted article.

7 ACKNOWLEDGEMENTS

This paper is based on the doctoral research conducted by the first author and supervised by the second one. The authors gratefully acknowledge financial support from Anglo American, and logistic support from DRD Gold, Gold Fields, and Sibanye Stillwater.

8 REFERENCES

Alonso, E.E., & Gens, A. (2006). Aznalcóllar dam failure. Part 1: Field observations and material properties. Géotechnique, 56(3), 165-183.

ASTM. (2015). ASTM D1587M-15 Standard practice for thin-walled tube sampling of fine-grained soils for geotechnical purposes.

ASTM. (2021). ASTM D7928-21 Standard Test Method for Particle-Size Distribution (Gradation) of Fine-Grained Soils Using the Sedimentation (Hydrometer) Analysis.

Ayala, J., Fourie, A., & Reid, D. (2022). Improved cone penetration test predictions of the state parameter of loose mine tailings. Canadian Geotechnical Journal.

Bandini, V., & Coop, M.R. (2011) The influence of particle breakage on the location of the critical state line of sands. Soils and Foundations, 51(4), 591-600.

Been, K., & Jefferies, M. (1985). A state parameter for sands. Géotechnique, 35(2), 99-112.

Been, K., & Olivera, R. (2016). Appendix B: Laboratory testing to determine the critical state of sands. In M. Jefferies, & K. Been, Soil Liquefaction - A Critical State Approach. CRC Press.

Been, K., Crooks, J., Becker, D., & Jefferies, M. (1986). The cone penetration test in sands: part I, state parameter interpretation. Géotechnique, 36(2).

Been, K., Jefferies, M., Crooks, J., & Rothenburg, L. (1987). The cone penetration test in sands: part II, general inference of state. Géotechnique, 37(3).

Been, K., Lingnau, B., Crooks, J., & Leach, B. (1987). Cone penetration test calibration for Erksak (Beaufort Sea) sand. Canadian Geotechnical Journal, 24(4).

Blight, G. (2010). Geotechnical Engineering for Mine Waste Storage Facilities. CRC Press.

Boulanger, R., & DeJong, J. (2018). Inverse filtering procedure to correct cone penetration data for thin-layer and transition effects. Cone Penetration Testing 2018. Delft, The Netherlands: CRC Press.

BSI. (1990). BS 1377-2 Methods of test for soils for civil engineering purposes - Classification tests.

Carrera, A., Coop, M., & Lancellota, R. (2011). Influence of grading on the mechanical behaviour of Stava tailings. Géotechnique, 61(11), 935-946.

Chang, H. (2009). The effect of fabric on the behaviour of gold tailings. PhD Thesis, University of Pretoria.

CIMNE. (2021). Computational analyses of Dam I failure at the Corrego de Feijao mine in Brumadinho.

da Fonseca, A., Cordeiro, D., & Molina-Gómez, F. (2021). Recommended procedures to assess critical state locus from triaxial tests in cohesionless remoulded samples. Geotechnics, 1(1), 95-127.

da Fonseca, A., Cordeiro, D., Molina-Gómez, F., & Fonseca, A. (2020). Annex 1: New site investigation and experimental campaign [IN PORTUGUESE]. *In* CIMNE, Computational analyses of Dam I failure at the Corrego de Feijao mine in Brumadinho.

Fourie, A., Verdugo, R., Bjelkevik, A., Torres-Cruz, L., & Znidarcic, D. (2022). Geotechnics of mine tailings: a 2022 State of the Art. In Rahman, & Jaksa (Ed.), Proceedings of the 20th ICSMGE-State of the Art and Invited Lectures (pp. 121-183). Sydney, Australia: Australian Geomechanics Society.

Høeg, K., Dyvik, R., & Sandbækken, G. (2000). Strength of undisturbed versus reconstituted silt and silty sand specimens. Journal of Geotechnical and Geoenvironmental Engineering, 126(7), 606-617.

Huntsman, S. (1985). Determination of in-situ lateral pressure of cohesionless soils by static cone penetrometer. PhD Thesis. University of California, Berkeley.

ICOLD (2025). Tailings Dam Safety: Bulletin 194. CRC Press/Balkema.

Jacobsz, S., & Narainsamy, Y. (2022). Field and laboratory research into the undrained behaviour of tailings at the University of Pretoria. J. of the Southern African Inst. of Mining and Metallurgy, 122(6), 267-273.

Jamiolkowski, M. (2014). Soil mechanics and the observational method: challenges at the Zelazny Most copper tailings disposal facility. Géotechnique, 64(8), 590-619.

Jefferies, M., & Been, K. (2016). Soil Liquefaction - A critical state approach, Second edition. CRC Press.

Jefferies, M., Morgenstern, N., Van Zyl, D., & Wates, J. (2019). Report on NTSF Embankment Failure. Cadia Valley Operations for Ashurst Australia.

Jung, H., Lin, J., & Stark, T. (2025). Sand state parameter from CPT. Canadian Geotechnical J., 62, 1-16.

McPhail, G., & Wagner, J. (1987). Disposal of Residues. *In* The extractive metallurgy of gold in South Africa.

Morgenstern, N., Vick, S., Viotti, C., & Watts, B. (2016). Report on the Immediate Causes of the Failure of

494 the Fundão Dam.
495 Mozaffari, M., & Ghafghazi, M. (2024). Material-specific interpretation of the state parameter from
496 drained cone penetration test. Canadian Geotechnical Journal, 61(12), 2858-2872.
497 Olson, S.M., & Stark, T.D. (2002). Liquefied strength ratio from liquefaction flow failure case histories.
498 Canadian Geotechnical Journal, 39(3), 629-647.
499 Olson, S.M., & Stark, T.D. (2003). Yield strength ratio and liquefaction analysis of slopes and
500 embankments. Journal of Geotechnical and Geoenvironmental Engineering, 129(8), 727-737.
501 Plewes, H., Davies, M., & Jefferies, M. (1992). CPT based screening procedure for evaluating liquefaction
502 susceptibility. Proceedings of the 45th Canadian Geotechnical Conference. Toronto, Canada.
503 Read, C. (1920). Logic: Deductive and Inductive. London: Simkin, Marshall.
504 Reid, D., & Fanni, R. (2022). A comparison of intact and reconstituted samples of a silt tailings.
505 Géotechnique, 72(2), 176-188.
506 Reid, D., Fanni, R., Koh, K., & Orea, I. (2018a). Characterisation of a subaqueously deposited silt iron ore
507 tailings. Géotechnique Letters, 8(4), 278-283.
508 Reid, D., Fourie, A., & Russell, A. (2018b). Effects of desiccation on shear strength of tailings – comparison
509 of clayey and sandy tailings. Proceedings of Tailings and Mine Waste, 2018.
510 Reid, D., Fourie, A., Castro, J., & Lupo, J. (2018c). Undrained shear strength evolution with loading on an
511 undisturbed block sample of desiccated gold tailings. Proceedings of Tailings and Mine Waste, 2018.
512 Reid, D., Fourie, A., & Fanni, R. (2022). Layering – the missing factor in fabric studies? Proc. of the 20th Int.
513 Conf. on Soil Mechanics and Geot. Eng.. Sydney, Australia: Australian Geomechanics Society.
514 Rezende, V. (2013). Study of the Behavior of a Sand Tailings Dam Constructed Using the Upstream Method
515 [IN PORTUGUESE]. PhD Thesis, Federal University of Ouro Preto.
516 Robertson, P.K. (2016). Cone penetration test (CPT)-based soil behaviour type (SBT) classification system
517 – an update. Canadian Geotechnical Journal, 53(12), 1910-1927.

Robertson, P.K. (2022). Evaluation of flow liquefaction and liquefied strength using the cone penetration test: an update. J. of Geot. and Geoenv. Engineering, 136(6), 842-853.

Robertson, P., de Melo, L., Williams, D., & Wilson, G. (2019). Report of the expert panel on the technical causes of the failure of Feijao Dam I.

Sadrekarimi, A. (2014). Effect of the mode of shear on static liquefaction analysis. Journal of Geotechnical and Geoenvironmental Engineering, 140(12).

Sadrekarimi, A., & Olson S.M. (2011). Critical state friction angle of sands. Géotechnique, 61(9), 771-783.

Schnaid, F. (2020). The Ninth James K. Mitchell Lecture: On The Geomechanics and Geocharacterization of Tailings. Proc. of the 6th Int. Conf. on Geot. and Geophysical Site Characterization. Edited by J.K. Mitchell. London, UK: Int. Soc. for Soil Mechanics and Geot. Eng.

Shuttle, D., & Cunning, J. (2007). Liquefaction potential of silts from CPTu. Canadian Geot. J., 44(1), 1-19.

Shuttle, D., & Jefferies, M. (1998). Dimensionless and unbiased CPT interpretation in sand. International Journal for Numerical and Analytical Methods in Geomechanics, 22(5), 351-391.

Shuttle, D., & Jefferies, M. (2016). Determining silt state from CPTu. Geotechnical Research, 3(3), 90-118.

Shuttle, D., Marinelli, F., Brasile, S., & Jefferies, M. (2022). Validation of computational liquefaction for tailings: Tar Island slump. Geotechnical Research, 9(1), 32-55.

Small, A., Witte, A., & Bjelkevik, A. (2024). What could tailings facility engineering look like in 2030? *In* Proceedings of Tailings and Mine Waste 2024. Colorado, USA.

Tehrani, F., Arshad, M., Prezzi, M., & Salgado, R. (2017). Physical Modeling of Cone Penetration in Layered Sand. Journal of Geotechnical and Geoenvironmental Engineering, 144(1).

Thevanayagam, S., Shenthan, T., Mohan, S., & Liang, J. (2002). Undrained Fragility of Clean Sands, Silty Sands, and Sandy Silts. Journal of Geotechnical and Geoenvironmental Engineering, 128(10).

Torres-Cruz, L. (2019). Limit void ratios and steady-state line of non-plastic soils. Proceedings of the Institution of Civil Engineers – Geotechnical Engineering, 172(3), 283-295.

542 Torres-Cruz, L. (2021). The Plewes method: A word of caution. Mining, Met. & Explor., 38, 1329-1338.

543 Torres-Cruz, L., & Santamarina, J. (2020). The critical state line of nonplastic tailings. Canadian

544 Geotechnical Journal, 57(10), 1508-1517.

545 UP (2023). University of Pretoria, in collaboration with Anglo American, launches state of the art mobile

546 soils testing laboratory for tailings engineering. https://www.up.ac.za/civil-

547 engineering/news/post_3191367-university-of-pretoria-in-collaboration-with-anglo-american-launches-

548 state-of-the-art-mobile-soils-testing-laboratory-for-tailings-engineering. *Accessed:* 07 September 2025.

549 Vermeulen, N. (2001). The composition and state of gold tailings. University of Pretoria, PhD Thesis.

550 Vick, S. (1990). Planning, Design, and Analysis of Tailings Dams. BiTech Publishers.